Clinical Cancer Research

Phase I Hepatic Immunotherapy for Metastases Study of Intra-Arterial Chimeric Antigen Receptor–Modified T-cell Therapy for CEA$^+$ Liver Metastases

Steven C. Katz[1], Rachel A. Burga[1], Elise McCormack[2], Li Juan Wang[3], Wesley Mooring[3], Gary R. Point[1], Pranay D. Khare[4], Mitchell Thorn[1], Qiangzhong Ma[2], Brian F. Stainken[5], Earle O. Assanah[5], Robin Davies[4], N. Joseph Espat[1], and Richard P. Junghans[2]

Abstract

Purpose: Chimeric antigen receptor–modified T cells (CAR-T) have demonstrated encouraging results in early-phase clinical trials. Successful adaptation of CAR-T technology for CEA-expressing adenocarcinoma liver metastases, a major cause of death in patients with gastrointestinal cancers, has yet to be achieved. We sought to test intrahepatic delivery of anti-CEA CAR-T through percutaneous hepatic artery infusions (HAIs).

Experimental Design: We conducted a phase I trial to test HAI of CAR-T in patients with CEA$^+$ liver metastases. Six patients completed the protocol, and 3 received anti-CEA CAR-T HAIs alone in dose-escalation fashion (10^8, 10^9, and 10^{10} cells). We treated an additional 3 patients with the maximum planned CAR-T HAI dose (10^{10} cells $\times$ 3) along with systemic IL2 support.

Results: Four patients had more than 10 liver metastases, and patients received a mean of 2.5 lines of conventional systemic therapy before enrollment. No patient suffered a grade 3 or 4 adverse event related to the CAR-T HAIs. One patient remains alive with stable disease at 23 months following CAR-T HAI, and 5 patients died of progressive disease. Among the patients in the cohort that received systemic IL2 support, CEA levels decreased 37% (range, 19%–48%) from baseline. Biopsies demonstrated an increase in liver metastasis necrosis or fibrosis in 4 of 6 patients. Elevated serum IFNγ levels correlated with IL2 administration and CEA decreases.

Conclusions: We have demonstrated the safety of anti-CEA CAR-T HAIs with encouraging signals of clinical activity in a heavily pretreated population with large tumor burdens. Further clinical testing of CAR-T HAIs for liver metastases is warranted. *Clin Cancer Res; 21(14); 3149–59. ©2015 AACR.*

Introduction

Liver metastases are a significant cause of morbidity and mortality in patients with gastrointestinal adenocarcinoma. Tumor infiltrating lymphocyte (TIL) studies have revealed that host T-cell responses to liver metastases are significant correlates of survival (1–5). Although those who mount effective immune responses to liver metastases tend to have prolonged survival, the vast majority of patients succumb to their disease in the context of endogenous immune failure. The immunosuppressive nature of the intrahepatic milieu (6–9) may promote the development of liver metastases and contribute to aggressive disease biology. Given the favorable effects of robust liver TIL responses and the inherent suppressive nature of the intrahepatic space, delivery of highly specific T-cell products for the treatment of liver metastases is a rational approach.

T cells engineered with chimeric antigen receptors (CAR) to enable highly specific tumor recognition and killing have gained considerable attention (10–12). Reprogramming T cells with CAR genes provides an MHC-independent mechanism for docking with and lysing tumor cells. Such modified T cells have been alternatively termed "designer T cells," "T-bodies," or "CAR-T cells" (13–15). Carcinoembryonic antigen (CEA) is an attractive target for CAR-T treatment of adenocarcinoma liver metastases given high levels of CEA expression and the ability to measure CEA in serum (16, 17). Upon antigen recognition, anti-CEA CAR-Ts proliferate, produce cytokines, and kill target cells (18). Previous clinical studies, which evaluated systemic delivery of anti-CEA T cells for metastatic adenocarcinoma, demonstrated both promise and dose-limiting toxicity (19). To improve the tolerability of anti-CEA CAR-Ts for liver metastases in addition to enhancing tumor killing within the liver, we studied a regional delivery strategy.

Regional intra-arterial delivery of chemotherapy for liver metastases has been demonstrated to yield superior response rates and limited systemic morbidity (20). Prior reports of

[1]Department of Surgery, Roger Williams Medical Center, Providence, Rhode Island/Boston University School of Medicine, Boston, Massachusetts. [2]Department of Medicine, Roger Williams Medical Center, Providence, Rhode Island/Boston University School of Medicine, Boston, Massachusetts. [3]Department of Pathology, Roger Williams Medical Center, Providence, Rhode Island. [4]Roger Williams Medical Center, GMP Core Facility and Clinical Protocol Office, Providence, Rhode Island. [5]Department of Radiology, Roger Williams Medical Center, Providence, Rhode Island/Boston University School of Medicine, Boston, Massachusetts.

Note: Supplementary data for this article are available at Clinical Cancer Research Online (http://clincancerres.aacrjournals.org/).

Corresponding Author: Richard P. Junghans, Department of Medicine, Roger Williams Medical Center, 825 Chalkstone Avenue, Providence, RI 02908. Phone: 401-456-2484; Fax: 401-456-6708; E-mail: rjunghans@rwmc.org

doi: 10.1158/1078-0432.CCR-14-1421

Translational Relevance

Chimeric antigen receptor–modified T cells (CAR-T) are highly specific immunotherapeutic products designed to target specific tumor antigens. Liver metastases represent a significant cause of death in patients with adenocarcinoma. Inefficient intrahepatic delivery of CAR-T via systemic infusion may limit the effectiveness of CAR-T treatments for liver metastases. We conducted a phase I trial to test CAR-T hepatic artery infusions (HAIs) to determine if direct regional delivery of CAR-T to liver metastases is safe and associated with signals of clinical efficacy. As CAR-T HAIs were well tolerated and associated with evidence of tumor cell killing in our subjects, further clinical testing of this approach alone and in combinatorial fashion is warranted.

regionally infused adoptive cell therapy products have demonstrated the safety of this approach (21–25). We propose that hepatic artery infusion (HAI) of anti-CEA CAR-Ts will limit extrahepatic toxicity while optimizing efficacy for treatment of liver metastases. To test the safety and *in vivo* activity of anti-CEA CAR-Ts in patients with liver metastases, we conducted the phase I Hepatic Immunotherapy for Metastases (HITM) trial (NCT01373047). We utilized a second-generation anti-CEA CAR (18), containing the CD28 costimulatory and CD3ζ signaling domains. We treated an initial cohort with CAR-T HAI intrapatient dose escalations without IL2 support and a second cohort that received fixed CAR-T doses with continuous IL2 infusions.

Six patients with liver metastases completed our protocol and we demonstrated that HAIs of anti-CEA CAR-Ts were well tolerated with and without IL2 infusion. We also demonstrated *in vivo* activity of CAR-T HAIs in patients with large volume liver metastasis refractory to conventional treatment. In addition to exploring the safety and efficacy of CAR-T HAIs, we examined immunologic correlates of intrahepatic and systemic responses. Our findings support testing of CAR-T HAIs for liver metastases in future trials.

Materials and Methods

Study design

In this phase I study (NCT01373047, RWH 11-335-99) we treated two cohorts of 3 patients with anti-CEA CAR-T HAIs without or with systemic IL2 support (Fig. 1). Cohort 1 was treated with CAR-T HAIs in intrapatient dose escalation fashion (10^8, 10^9, and 10^{10} cells) without IL2. Those in the cohort 2 received 3 HAI of 10^{10} CAR-Ts in addition to continuous systemic IL2 infusion at 75,000 U/kg/d via an ambulatory infusion pump.

Eligible patients had measurable unresectable CEA-positive liver metastasis or detectable serum CEA levels and failed one or more lines of conventional systemic therapy. Minimal extra-hepatic disease in the lungs or abdomen was permitted. No commercial sponsor was involved in the study. Clinical assessments were scheduled on infusion days, and on days 1, 2, 4, and 7 postinfusion. Liver MRI and PET examinations were performed within 1 month before the first infusion and then within 1 month following the third CAR-T HAI. The study radiologist (B.F. Stainken) graded responses according to modified RECIST (mRECIST) and immune-related response criteria (26). Safety evaluation was performed per protocol. Severity of adverse events was graded using the National Cancer Institute Common Terminology Criteria for Adverse Events version 4.0. The study was performed after approval by the institutional review board of the Roger Williams Hospital in accordance with an assurance filed with and approved by the U.S. Department of Health and Human Services. Informed consent was obtained from each subject enrolled in the study.

Human CAR-T cell production

The second-generation anti-CEA scfv-CD28/CD3ζ (Tandem) CAR was cloned into the MFG retroviral backbone as previously described (FDA BB IND 10791; ref. 18). Briefly, the tandem molecule was generated by fusing the hMN14 sFv-CD8 hinge segment of the IgTCR (IgCEA) in the MFG retroviral backbone with a hybrid CD28/CD3ζ molecule. The construct was verified by sequencing. The clinical retroviral vector supernatant was produced using PG13 cells to generate gibbon ape leukemia virus pseudotyped viral particles as described (27). All clinical batches were prepared at Indiana University vector production facility (Indianapolis, IN) and stored at −80°C.

Rhode Island Blood Center personnel performed leukapheresis at the Roger Williams Medical Center (RWMC, Providence, RI). Anti-CEA CAR-Ts were prepared at the RWMC Cell Immunotherapy and Gene Therapy (CITGT) Good Manufacturing Practice (GMP) Facility with standard operating procedures (SOP) for processing, manufacturing, expansion, dose harvesting, labeling, storage, and distribution. Briefly, patient peripheral blood mononuclear cells (PBMC) were isolated from leukapheresis product using Ficoll (Sigma). We then activated PBMCs for 48 to 72 hours in tissue culture flasks (BD Falcon) containing AIM V media (Life Technologies) supplemented with 5% sterile human AB serum (Valley Biomedical), 50 ng/mL of anti-CD3 monoclonal antibody (OKT3; Ortho Biotech), and 3,000 U/mL of IL2 (Prometheus).

Using the spinoculation method (28), 7.2 to 14.4×10^8 T cells were transduced in retronectin (TaKaRa Bio Inc.) coated 6-well plates in AIM V media with 5% human AB serum, 3,000 U/mL of IL2, and protamine sulfate (MP Biomedicals) at low-speed centrifugation for 1 hour at room temperature. Three transductions were carried out over 24 hours. After transduction, cells were washed and incubated for 48 to 72 hours at 37°C. CAR-Ts were further expanded in Lifecell tissue culture bags (Baxter) for 10 to 14 days. CAR-T growth curves and cell viability were examined periodically and cell growth media were replaced as required. CAR-Ts were examined by flow cytometry with fluorescently labeled antibodies specific for CD3 (UCHT1; Invitrogen), CD4 (SK3; BD Biosciences), CD8 (3B5; Invitrogen), and CAR expression (WI2 antibody; Immunomedics). The WI2 antibody was prepared as an APC conjugate (WI2-APC; Molecular Probes). Flow cytometry was performed on a CyAn (Beckman Coulter) or LSR-II (BD Biosciences) machine. *In vitro* activity of patient products was measured by bioluminescence cytotoxicity assay. Luciferase-expressing CEA^+ tumor cells were mixed with anti-CEA CAR-T at various ratios in 96-well round bottom plates and loss of bioluminescence from each well measured (29).

We prepared clinical doses using a Fenwal cell harvester system (Baxter) in freezing media containing PlasmaLyte (Baxter), 20% human bovine albumin (Valley Biomedicals), 10% DMSO (Bioniche Pharma) and IL2. Bacterial and fungal cultures were monitored for 14 and 28 days, respectively. We performed assays for endotoxin with LAL Endotoxin assay kits (Lonza). The clinical dose was stored in liquid nitrogen and thawed immediately before infusion.

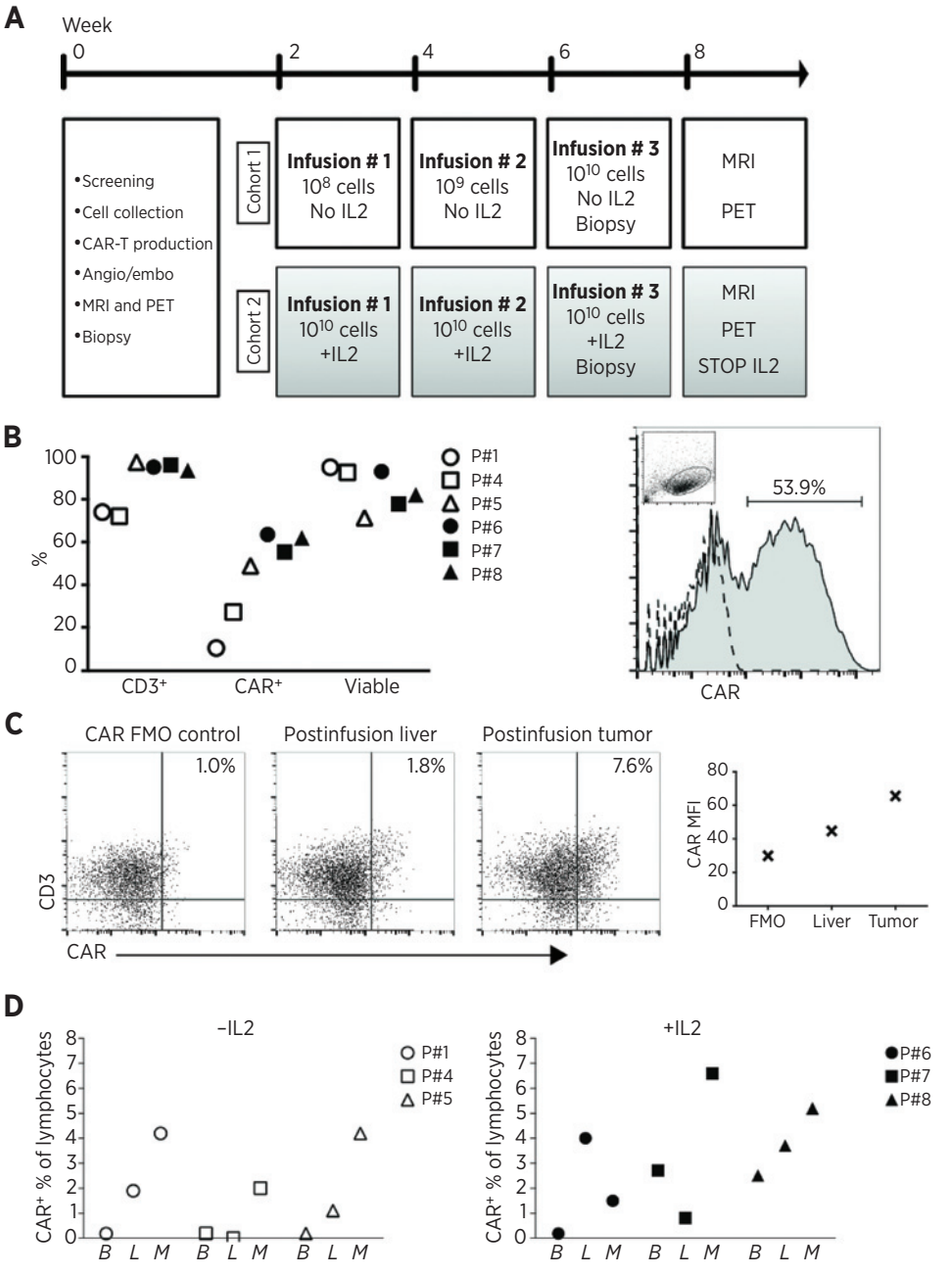

Figure 1.
HITM trial design and CAR-T cell trafficking data. A, patient treatment and evaluation schedule. B, quality control data for the CAR-T products is shown. The percentage of cells that expressed CD3 and the anti-CEA CAR, in addition to the viability fraction, are illustrated for each patient (left). Flow cytometry histogram of preinfusion product from patient 7 demonstrating CAR^+ percentage, with the dashed line representing the FMO control and lymphocyte gating demonstrated in the inset dot plot (right). C, flow cytometry data from HITM patient 7 to illustrate detection of $CD3^+CAR^+$ cells within normal liver and liver metastasis 2 weeks following the second CAR-T HAI. CAR gating was set based on the illustrated FMO control. Plot on right demonstrates CAR mean fluorescence intensity (MFI) values from each specimen for patient 7. D, blood (B), normal liver (L), and liver metastasis (M) biopsies were harvested and analyzed by flow cytometry as illustrated for patient 7. CAR-T percentages among lymphocytes are shown. Percentages were adjusted by subtracting background staining values obtained from FMO control samples. All values represent samples taken 2 weeks following the second infusion. The second dose for cohort 1, −IL2, was 10^9 cells and for cohort 2, +IL2, was 10^{10} cells.

Product delivery

At baseline, a mapping angiogram was performed via a common femoral artery approach. The gastroduodenal and right gastric arteries, in addition to other potential sources of extrahepatic perfusion, were embolized with microcoils. For CAR-T infusions, the same arterial access procedure was carried out and the cells were hand injected via a 60-mL syringe at a rate of <2 mL/second with a total volume of 100 mL. Angiography with calibrated contrast rate was performed after the first 50 mL and at completion of the CAR-T infusion to confirm preserved arterial flow. Infusions were delivered into the proper hepatic artery when possible. In cases of aberrant hepatic arterial anatomy, where either the right or left hepatic artery did not arise from the proper hepatic artery, the dose was split based upon lobar volume calculations. In such cases, split doses were delivered separately into the right and left hepatic arteries to ensure proportionate CAR-T delivery to both lobes.

Correlative studies

Normal liver and liver metastasis core needle (16-gauge) biopsies were obtained under sonographic guidance at baseline and at the time of the third CAR-T HAI. Three cores were obtained for normal liver and liver metastases, with each confirmed by cytology. For each case, 4- to 5-μm sections were stained with hematoxylin and eosin (H&E) and additional unstained slides were stained with anti-CEA antibody (TF 3H8-1; Ventana). All

Table 1. Patient characteristics

ID	Sex	Age	DX	Chemo	DFI	EHD	No. LM	Size (cm)	CEA (ng/mL)	IL2	CAR-T doses
1	F	54	Colon	4	0	None	>10	14.4	3,265	No	3
2	M	52	Colon	2	0	Lungs	>15	12.6	352	No	2[c]
3	M	52	Gastric	1	0	None	1	5.7	29.9	No	0[d]
4	M	55	Ampullary[a]	2	9	Lungs, RPN	1	1.7	362	No	3
5	M	63	Colon	3	37	None	2	5.7	2[b]	No	3
6	M	51	Colon	3	36	Lungs	>10	10.5	1,112	Yes	3
7	F	53	Colon	3	0	Lungs	>10	8.0	30	Yes	3
8	M	66	Colon	2	0	None	>10	9.8	72	Yes	3
		Mean = 57		Mean = 2.5				Mean = 8.4	Mean = 807.2		

Abbreviations: DFI, disease-free interval from diagnosis of primary to liver metastases; IL2, continuous IL2 infusion with CAR-T; LM, liver metastases; size, largest LM before CAR-T treatment; RPN, retroperitoneal nodes; CHEMO, number of lines of systemic therapy prior to enrollment.

[a]Pancreatobiliary subtype of ampullary carcinoma.

[b]CEA expression confirmed in tumor specimen by immunohistochemistry.

[c]Withdrew after 2 doses due to extrahepatic progression.

[d]Withdrew due to unrelated medical condition.

immunohistochemical stains were performed on the Ventana Medical System at Our Lady of Fatima Hospital (Providence, RI). All slides were reviewed in blinded fashion and graded for necrosis and fibrosis. Fibrosis was scored as follows: 0%, grade 0; 5% to 10%, grade 1; 11% to 50%, grade 2; >50%, grade 3. Necrosis was scored as follows: 0%, grade 0; 0% to 10%, grade 1; 11% to 50%, grade 2; >50%, grade 3. Flow cytometry was performed on fresh biopsy tissue for CAR-T cells and peripheral blood as described above.

We measured serum IFNγ levels in all patients by ELISA (eBioscience). Samples were purified with the Purelink DNA Isolation Kit (Life Technologies) according to the manufacturer's instructions. Patient serum was screened for anti-CAR antibodies 1 month after treatment by flow cytometry. We mixed CAR^+ or CAR- Jurkat cells with 100 μL of 1:1 diluted patient serum and then stained with secondary goat anti-human immunoglobulin.

CAR DNA was measured from patient whole-blood genomic DNA by qPCR performed at the Boston University Analytical Core Facility. SYBR Green technology was used and CAR-positive samples were identified using 100 μmol/L 28F2 forward (5′-GCAAGCATTACCAGCCCTAT-3′) and zr2 reverse (5′-GTTCTG-GCCCTGCTGGTA-3′) primers (custom, Sigma Aldrich). Plasmid DNA containing the CAR gene was used as a positive control qPCR. Additional primers were used to amplify CD3, GAPDH, and RPL13A (Bio-Rad). Raw cycle threshold (C_t) values were normalized to the average of the two reference genes (RPL13A and GAPDH) and we used the DeltaDelta C_t method to analyze the results. Wet-lab validated and MIQE-compliant primers were purchased from Bio-Rad.

Results

Study design and patient characteristics

We enrolled 8 patients with unresectable CEA^+ adenocarcinoma liver metastases who progressed on an average of 2.5 (range, 2–4) lines of conventional systemic therapy (Table 1). Six patients completed the protocol (Fig. 1A), 1 patient withdrew due to an unrelated infection before treatment, and another patient withdrew due to extrahepatic disease progression before his third CAR-T HAI. Of the patients that completed the protocol, 4 were male and 2 were female. Five patients had stage IV colorectal carcinoma and 1 patient had pancreatobiliary ampullary carcinoma. The average age was 57 (range, 51–66). Patients presented with substantial disease burdens, with the average size of the

Table 2. Adverse events

ID	IL2	Grade	*n*	Description
1	No	1	12	Fever, mylagias, abdominal pain, nausea, emesis, and tachycardia
		2	2	Abdominal wall muscle spasm and ↑ALT
		3	2	↑AST and ↑alk phos
4[a]		1	5	Ascites, edema, thrombocytopenia, ↑ALT, ↑AST
		2	5	↑alk phos, leukopenia, dyspnea
		3	2	Pleural effusion, anorexia
5		1	2	Fever, rash
		3	1	Emesis
6	Yes	1	5	↑AST, ↑ALT, thrombocytopenia, dyspnea, rash
		2	1	Lower extremity edema
		3	3	Emesis, subscapular liver hematoma, ↑alk phos
7		1	7	Eosinophilia, chills, fever, abdominal pain, ↑bilirubin
		2	2	Emesis, diarrhea
		3	3	Tachycardia with fever (104°F)[b], emesis, abdominal pain
8		2	6	Fever, tachycardia, diarrhea, dehydration, lower extremity edema
		3	3	Anemia, abdominal pain, colitis[b]

NOTE: Patient 2 experienced grade 3 abdominal pain and dehydration; he was taken off protocol after the second HAI and died due to disease progression 23 days later. Patient 3 was withdrawn before CAR-T infusion due to an unrelated medical condition.

Liver function test adverse events reflect values outside of normal range and not necessarily change from baseline.

[a]Death due to disease progression 28 days after third infusion.

[b]Led to IL2 dose reduction.

largest liver metastasis being 8.4 cm (range, 1.7–14.4) and 5 patients having more than 10 liver metastases. The mean CEA level upon enrollment was 807 ng/mL (range, 2–3,265). Five of 8 patients had synchronous colorectal liver metastases, and the mean disease-free interval was 27.3 months (range, 9–37) for patients with metachronous liver metastases. All further analyses include only the 6 patients who completed the study.

CAR-T cell product assessment

The leukapheresis product from each patient was analyzed by flow cytometry before and following transduction with anti-CEA CAR construct. For all patients, the mean percentage of $CD3^+$ cells following leukapheresis was 55% (range, 12.0–82.0) and increased to 91% (range, 72–97) following activation and transduction (Fig. 1B). The mean CD4:CD8 ratio was 2.4 (range, 1.4–4.7) in the leukapheresis samples and 0.8 (0.2–2.2) in the final products (not shown). The transduction efficiency (CAR^+) ranged from 10% to 64%, with a mean of 45% (Fig. 1B). Negligible FoxP3 staining was detected among CAR^+ T cells before infusion (not shown). Cells in the final products were 85% viable before infusion (range, 71–95). *In vitro* cytotoxicity assays confirmed that patient products specifically lysed CEA^+ target cells (Supplementary Fig. S1).

CAR-T cell trafficking following regional infusion

We obtained CT guided percutaneous biopsies to sample liver metastasis and normal liver before the first CAR-T HAI and at the time of the final HAI. The proportions of CAR-T (CAR^+/total lymphocyte %) in liver metastasis biopsy, normal liver biopsy, and peripheral blood samples were determined by flow cytometry. Samples from patient 7 demonstrated that 0.8% of normal liver mononuclear cells were CAR^+ following HAI of CAR-T and 6.6% of intratumoral mononuclear cells were CAR^+ (Fig. 1C). We confirmed that that CAR^+ cells in the postinfusion liver metastasis biopsy specimen were $CD3^+$. CAR-T population data in peripheral blood, normal liver, and liver metastases are shown for all patients (Supplementary Fig. S2, Fig. 1D). CAR-Ts were more abundant in the liver metastases compared with normal liver in 5 of 6 patients. In patient 5, CAR-T were found to comprise 2.0 % of liver metastasis mononuclear cells in a sample obtained during a microwave ablation procedure 12 weeks following his final CAR-T infusion (not shown). In 4 patients, CAR-T were not detectable in peripheral blood but were transiently present in patient 7 and patient 8 at the time of the final infusion, and the levels dropped below detection 3 days later. We also performed qPCR on peripheral blood samples taken at day 2 following the final infusion; only patient 7 had a measurable increase (1.1-fold) in CAR DNA relative to baseline (not shown).

Anti-CAR antibodies were not detected in patient sera 1 month following CAR-T infusion. This was confirmed by screening sera against CAR^+ and CAR^- target cells and staining for anti-human Ig on the CAR^+ cells as described in the methods section.

Safety data

Adverse events (AE) of any grade attributable to any cause were observed in all patients who completed the trial (Table 2). The dose in cohort 1 reached the planned maximal HAI CAR-T infusion level at 10^{10} cells. No CAR-T dose reductions were required in cohort 1 and, therefore, all patients in cohort 2 received 3 doses at the 10^{10} level with IL2 support. There were no grade 4 or 5 adverse events. Febrile AEs were observed in 4 patients. Patient 7 experienced grade 3 fever and tachycardia, with a temperature peak of 104°F. The fever and tachycardia resolved in patient 7 after a 50% dose reduction in her systemic IL2 infusion. Of note, patient 7 also experienced an increase in her peripheral eosinophil count with a peak of 20% and absolute count of 3,740 per mL. Given the reported association between IL2 infusion and cardiac thrombosis with other features of Loeffler syndrome (30), we obtained an echocardiogram and electrocardiogram that were normal. The eosinophil count returned to normal limits without specific intervention.

Normal liver parenchyma and biliary structures were well preserved following CAR-T HAIs. Biopsies from normal liver did not demonstrate increased levels of inflammation or fibrosis following CAR-T HAI whether or not systemic IL2 was administered (Fig. 2A). Although all patients experienced transient elevations of alkaline phosphatase (alk phos), total bilirubin, and aspartate aminotransferase levels (AST), only patient 1 experienced grade 3 elevations and the majority of values did not deviate significantly from baseline levels (Fig. 2B). Portal pressures and liver synthetic function were not adversely affected by the CAR-T HAIs, as reflected by no patient becoming thrombocytopenic (Fig. 2C) or coagulopathic (Fig. 2D).

Clinical activity

At last follow-up, 5 of the 6 heavily pretreated patients who completed the trial died due to disease progression (Table 3). MRI and PET scans were performed in 5 of 6 patients at baseline and 2 to 4 weeks following the third CAR-T HAI. Patient 8 did not obtain final imaging following a return to his native country and ultimately died of disease progression. All patients except patient 5 were determined to have radiographic disease progression. Patient 5 was found to have stable disease by MRI and PET (Supplementary Fig. S3A, arrow). Patient 7 developed new lesions and demonstrated an increase in size of some preexisting lesions, whereas other lesions decreased in size. The lesion in the posterior sector of patient 7 that decreased in size on MRI was not visible on PET (Supplementary Fig. S3B). More medial disease that was decreased in size on MRI was noted to become hypometabolic on the postinfusion PET for patient 7.

As we anticipated limited utility for short follow-up conventional imaging following infusion of CAR-T, we measured serum CEA levels at multiple time points following each of the three HAIs for each patient. Among the patients in cohort 1, transient decreases in serum CEA were demonstrated in 2 patients following each CAR-T HAI (Fig. 3A). CEA kinetics were closely paralleled by changes in serum CA19-9 levels (not shown). Patient 4, who presented with hepatobiliary subtype ampullary carcinoma, was the only patient without a CEA decrease at any point during the trial and he also had the shortest survival time.

The patients in cohort 2 who received systemic IL2 along with anti-CEA CAR-T had more favorable CEA responses to treatment. As each of the three patients in cohort 2 required an IL2 interruption or dose reduction, which would likely impact CAR-T function, we compared CEA levels at baseline with the time point just before IL2 dose change. When using these time points, all 3 patients in cohort 2 had decreases in serum CEA concentrations (Fig. 3A and Table 3). Patients 7 and 8 had a 48% and 43%

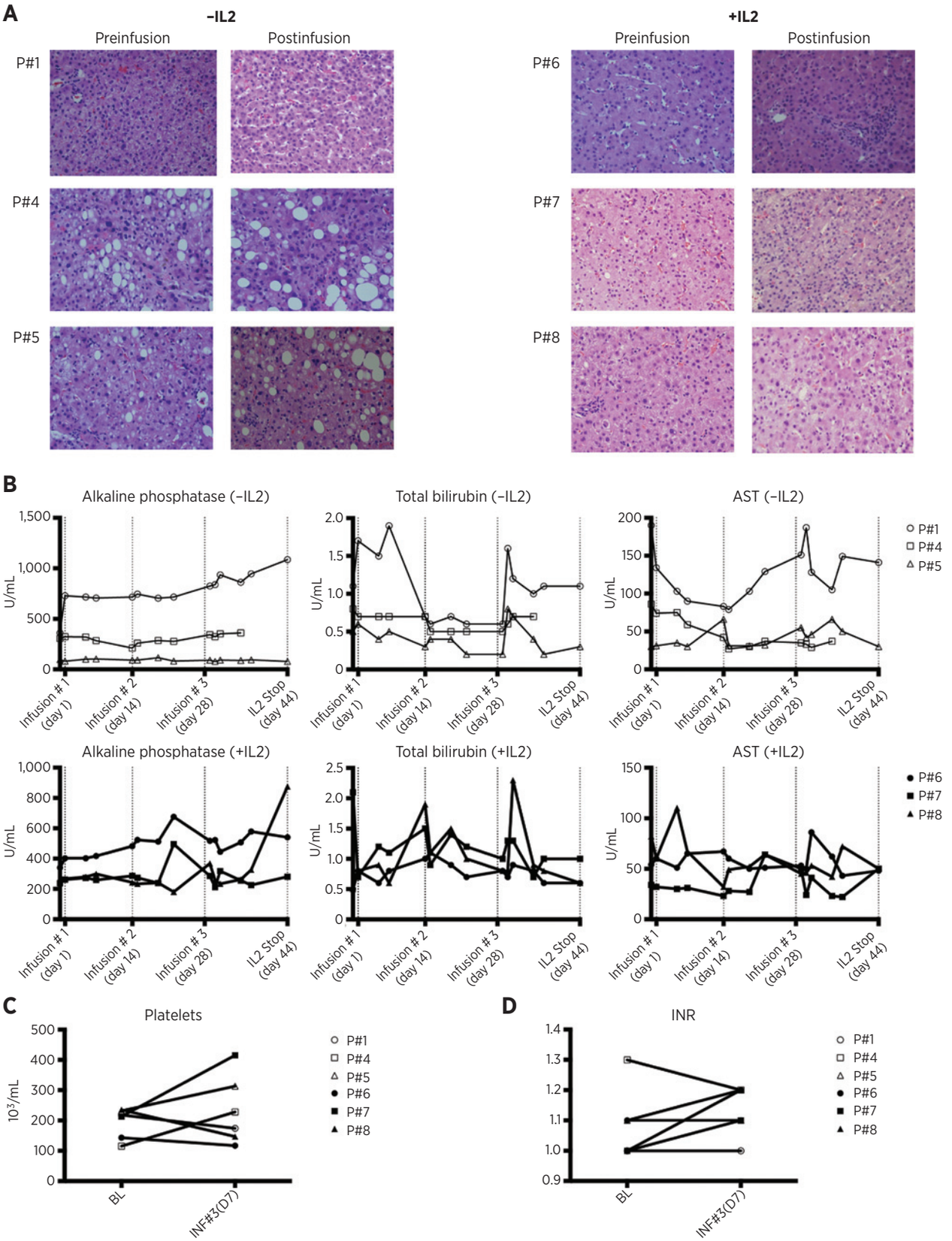

Table 3. Patient outcomes

ID	IL2	CAR$^+$%	MRI	PET	ΔCEA%[a]	OS (wks)	Status
1	No	10.4	PD	PD	−1	30	DOD
4	No	27.2			+401	8	DOD
5	No	48.9	SD	SD	+63	102	AWD—residual disease treated with microwave ablation and further systemic therapy
6	Yes	63.5	PD	PD	−19	13.0	DOD
7	Yes	57.4	PD	PD	−48	17	DOD—underwent resection of obstructing primary right colon tumor after final CAR-T infusion
8	Yes	61.9	PD	PD	−43	19	DOD

NOTE: Patient 2 withdrawn after 2 CAR-T doses due to extrahepatic progression and was DOD 23 days after second CAR-T infusion. Patient 3 withdrawn after cell collection due to unrelated medical condition.

Abbreviations: AWD, alive with disease; DOD, dead of disease; PD, progressive disease; SAE, serious adverse events; SD, stable disease.

[a]Fold change from baseline at time of second biopsy or IL2 infusion disruption.

decrease in serum CEA concentrations, respectively, before IL2 dose interruption or reduction. The mean overall survival time for the 6 patients who completed the trial was 30 weeks with a median of 15 weeks (range, 8–102). Patient 5 is alive with disease at 23 months (102 weeks) following his final CAR-T HAI. Following completion of the HITM trial, patient 5 was determined to have stable disease and we performed a microwave ablation of residual unresectable tumor (Supplementary Fig. S3).

Detecting radiographic responses in heavily pretreated patients with advanced metastatic disease is challenging, and even more so with immunotherapy where intratumoral inflammation and edema may minimize the relevance of standard RECIST criteria (26). As such, we obtained liver metastasis biopsies before and following CAR-T HAIs to assess degrees of intratumoral necrosis and fibrosis. After review by a blinded pathologist, 4 patients had an increase in intratumoral fibrosis and 3 patients were scored as having an increase in necrosis within their liver metastases (Fig. 3B). An increase in liver metastasis fibrosis is demonstrated for patient 1 and a decrease in CEA$^+$ tumor cells by immunohistochemistry for patient 8 (Fig. 3C).

Serum IFNγ concentrations and CEA responses correlate with IL2 administration

We measured serum IFNγ levels by ELISA at multiple time points. Spikes in IFNγ were noted to occur 24 to 48 hours after doses in all patients, without or with systemic IL2 (Supplementary Fig. S4). Serum CEA changes were compared with peak change in IFNγ for each patient (Fig. 3D, top). The inverse correlation between peak IFNγ levels and CEA change was significant ($R = -0.94$; $P = 0.02$). All patient HAI CAR-T doses contained a quantity of IL2 (600,000 U). The three patients (6, 7, and 8) with continuous systemic IL2 exposure and largest CAR-T doses had the best CEA responses and the highest mean IFNγ levels ($P = 0.03$, Fig. 3D, bottom).

Discussion

Our interest in immunotherapy for liver metastases is based upon studies that have demonstrated liver metastasis patients with robust T-cell responses have significantly improved outcomes. However, most liver metastasis patients fail to mount effective intrahepatic antitumor immunity (1). CAR-T technology has advanced considerably in recent years and holds tremendous promise (10, 11) as an immunotherapeutic tool. We chose HAI of CAR-T to minimize immune-mediated damage to CEA-expressing extrahepatic tissues and based upon the favorable therapeutic index of chemotherapy HAIs (20, 31). We established the safety of anti-CEA CAR-T HAIs with and without systemic IL2 support, reaching the maximum planned dose of 10^{10} cells. Systemic IL2 support was associated with increased serum IFNγ levels and improved CEA responses, at the expense of more severe but manageable adverse events. Although there were no radiographic partial or complete responses, 1 of 6 patients had stable disease and is alive at 23 months follow-up. Importantly, histologic evidence of increased liver metastasis necrosis and fibrosis were seen in the majority of subjects following CAR-T HAI.

The safety of CAR-T HAIs is in line with reports from other groups (21, 23, 25, 32) that infused non-CAR cellular products into the hepatic circulation. The limited systemic exposure of CAR-T in our study subjects likely accounted for the favorable adverse event profile. HAI led to preferential accumulation of CAR-T within liver metastases in 5 of 6 HITM patients, compared with normal liver and peripheral blood. CAR-Ts were not detected in the peripheral blood in 4 of 6 patients and only transiently in patients 7 and 8. Moderate elevations of liver function test values were likely related to the CAR-T HAI but did not result in clinically significant consequences. Systemic infusion of T cells expressing anti-CEA TCR was reported to result in dose-limiting toxicity (19). Similar toxicities have been seen with our CAR-T when systemically infused, particularly with IL2 support (R.P. Junghans;

Figure 2.

Assessment of liver inflammation and injury following anti-CEA CAR-T HAIs. A, normal liver biopsies were obtained under CT guidance before the first infusion and just before the third infusion. Routine H&E staining is shown. B, alkaline phosphatase, total bilirubin, and aspartate aminotransferase levels are shown for the patients who did not or did receive systemic IL2. Dotted vertical lines, CAR-T infusion time points and the first data point represents the baseline value before CAR-T infusion. Platelet counts (C) and INR values (D) for each patient are shown.

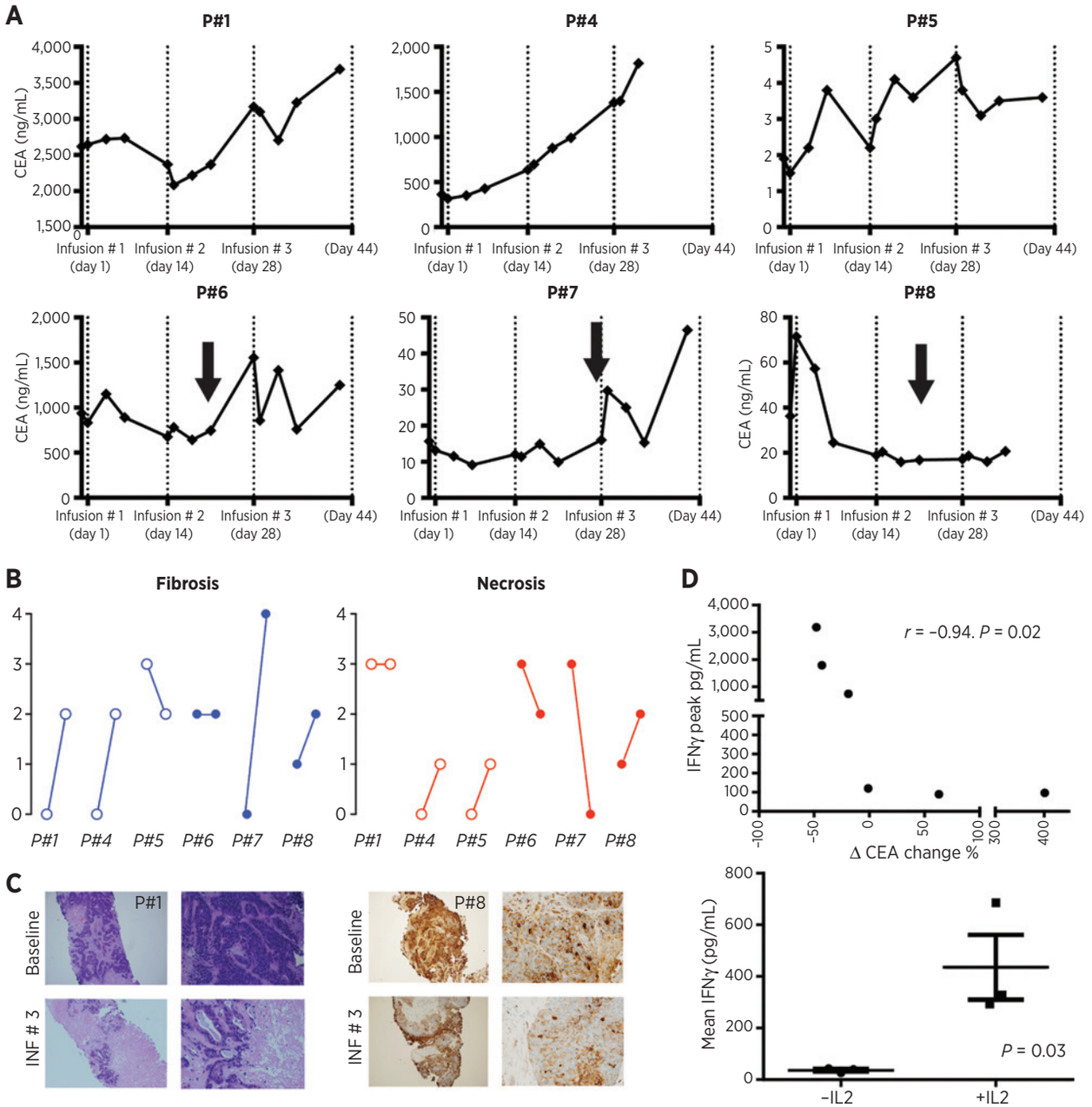

Figure 3.
Assessments of clinical activity of anti-CEA CAR-T HAIs. A, serum CEA levels are illustrated for patients who were treated with CAR-T HAIs alone (top row) or CAR-T with systemic IL2 support (bottom row). CAR-T infusion time points are indicated by dotted vertical lines and IL2 dose interruptions by black arrows. The first data point represents the baseline value before CAR-T infusion. B, a blinded pathologist, comparing baseline to postinfusion, scored fibrosis and necrosis from normal and liver metastasis biopsies. For each patient, baseline and postinfusion scores are shown from left to right. C, routine H&E staining for patient 1 (left) and CEA staining for patient 8 (right) are shown, comparing baseline with postinfusion. D, we measured serum IFNγ concentrations by ELISA before and after each hepatic artery CAR-T infusion. Peak IFNγ levels were correlated with the percentage change in CEA concentration from baseline to the time point before IL2 dose interruptions or reductions (top). Mean IFNγ values were calculated for each patient and compared among those who did or did not receive systemic IL2 support in addition to hepatic artery CAR-T infusions (bottom).

unpublished data). Our continuous ambulatory infusion dose of IL2, 75,000 U/kg/d, is several-fold lower than what is given in other protocols (33). Despite the low daily dose of the IL2 in this study, 2 patients experienced grade 3 events requiring IL2 dose reductions. We attributed these adverse events, including severe pyrexia and colitis, to the IL2 based upon the fact that the symptoms resolved promptly upon IL2 dose reduction. We cannot completely exclude the possibility that the IL2 activated a small number of systemically circulating anti-CEA CAR-T that mediated fever and colitis. Overall, our IL2 infusion strategy was

well tolerated and the adverse events easily managed by dose reductions.

MRI and PET scans did not demonstrate a response in any patient, while 1 patient had stable disease and is alive more than 23 months following his final CAR-T HAI. Our patients were heavily pretreated with profound disease burdens, with 4 of 6 patients presenting with more than 10 liver metastases. Due to rapid disease progression following cessation of CAR-T infusions and IL2, we were unable to follow 5 of the 6 patients beyond 2 months, when responses to immunotherapy may manifest radiographically (26). We are encouraged by the CEA responses in the cohort that received IL2 and by the evidence of necrosis and fibrosis following CAR-T HAI in several patients. Based on the timing of the biopsies, we cannot determine if IL2 alone or IL2 in combination with a higher CAR-T dose in cohort 2 contributed to histologic findings (34). We also cannot reach definitive conclusions about the efficacy of our approach, but speculate that responses would be more favorable in patients with lower disease burdens. Interestingly, CEA declines may be inherently beneficial given the recently reported proangiogenic effects of CEA (35).

To assess trafficking, we performed image-guided core biopsies of pre- and postinfusion liver metastases and surrounding liver. We analyzed biopsy specimens for CAR^+ cells and studied the cell populations by flow cytometry. CAR^+ T cells were present in detectable numbers in both tumor and normal liver after HAI, with numbers passing through liver being undetectable or only minimally detectable in peripheral blood. Similarly, in a parallel study with systemic administration of the same anti-CEA CAR-T, we demonstrated the presence of CAR^+ cells by immunohistochemistry in normal liver and in tumor after infusion (Junghans and colleagues; data not shown), thus confirming trafficking by this independent method.

As to intrahepatic T-cell distribution after HAI, Takayama and colleagues found a preferential localization in tumor versus normal liver after infusion of radiolabeled tumor infiltrating lymphocytes (TIL; ref. 36). Our own flow cytometric analyses of core specimens in this study are also consistent with a conclusion of preferential tumor distribution of CAR T cells in 4 of 6 subjects after HAI. However, further directed assessments will be required to independently confirm this association on a statistical level.

Performing detailed assessments of CAR-T phenotype and function can be challenging when working with a small subpopulation of mononuclear cells isolated from core need biopsy specimens. Given the technical limitations related to detecting CAR-T in liver biopsies following infusion, alternative strategies, including molecular imaging with MRI or PET scans (37), or radiolabeling as done by Takayama and colleagues (36) above, should receive consideration for future trials.

Effective delivery of anti-CEA CAR-T to CEA^+ tumor deposits also correlated with histologic evidence of tumor killing and serum cytokine surges (38). CEA responses were noted in 3 patients, all of whom received systemic IL2. IL2 alone is not expected to affect CEA levels, which presumptively implicates this fraction of CAR-T cells that traffic to tumor as mediating this effect. Prior work in this laboratory has shown tumor responses in animals (34) and in humans (Junghans and colleagues; unpublished results) with CAR-T cells that are dependent upon IL2 supplementation.

One potential limitation on the activity of CAR-T *in vivo* would be the development of anti-CAR antibodies that could lead to rapid elimination of CAR^+ cells. In the present instance, no patient developed an anti-CAR response. In many cases, the CAR includes foreign protein with a murine antibody domain that can elicit an immune response. In the current anti-CEA CAR, however, a CDR-grafted humanized version of the murine MN14 antibody (39) was selected for CAR engineering; such humanized antibodies are known to have much reduced immunization potential with only 4% incidence of anti-immunoglobulin responses in human clinical trials (40). Thus, the absence of anti-CAR antibody reaction in our patients is reassuring but not surprising.

We speculate that improved CAR-T delivery by HAI may decrease the need for lymphodepleting or myeloablative preconditioning (41). In the absence of preconditioning or enhanced cytokine support strategies, multiple CAR-T HAI doses will be necessary. As such, defining surrogates of early response will be important to identify patients who are likely to benefit from serial CAR-T HAIs. Intratumoral necrosis and fibrosis are meaningful correlates of antitumor efficacy, but obtaining liver biopsies at multiple time points is not without risk.

IFNγ correlated with CEA response in the present study. Whereas IL2 likely directly affected systemic IFNγ levels (42), activation of CAR-T within the liver may have also contributed to IFNγ surges. Of note, HAI of CAR-T also led to an increase in serum levels of IL6 and IL17 in patients who did and did not receive IL2 (38), suggesting that CAR-T activity in the intrahepatic space can be detected by peripheral cytokine changes. Increases in serum IFNγ were also noted in the cohort 1 patients, who received an initial HAI bolus of IL2 with their CAR-T doses. This was more prominent in cohort 2 patients with sustained systemic IL2 exposures, in addition to higher CAR-T doses. These findings are compatible with a systemic IL2 effect on T-cell IFNγ production. Interestingly, the highest IFNγ levels in patient 1 and patient 5 were noted after the maximal CAR-T dose (10^{10}). CAR-T that were activated by CEA^+ tumor were also likely to have contributed to increases in serum IFNγ. Our study design does not permit us to conclude that IFNγ changes were solely related to CAR-T activity. Even so, serum IFNγ is an attractive candidate biomarker of clinical responsiveness to CAR-T HAI for liver metastases.

We propose that addressing immunosuppression within the intrahepatic space can enhance the clinical efficacy of CAR-T HAIs (6–8, 43, 44). Based on our findings, further clinical study of CAR-T HAIs is warranted to establish an optimal combinatorial approach. Checkpoint blockade antibodies are an attractive option for use in combination with CAR-T HAIs (45, 46). Immune checkpoint blockade is particularly appealing given that we have found high levels of PD-L1 expression among suppressive liver immune cells, along with PD-1 expression among anti-CEA CAR-T (S.C. Katz; unpublished data). Finally, future HAI CAR-T trials may include alternative methods of CAR-T expansion, including activation with anti-CD3/CD28-coated beads (11, 47). The results from our initial phase I HITM trial demonstrate the safety of CAR-T HAIs and encouraging signals of clinical activity. CAR-T HAIs may prove to be a valuable component of a combinatorial immunotherapeutic approach for liver metastasis refractory to conventional treatments.

Disclosure of Potential Conflicts of Interest

S.C. Katz is a consultant/advisory board member for InCytu and SureFire Medical. No potential conflicts of interest were disclosed by the other authors.

Authors' Contributions

Conception and design: S.C. Katz, N.J. Espat, R.P. Junghans
Development of methodology: S.C. Katz, P.D. Khare, Q. Ma, B.F. Stainken, N.J. Espat, R.P. Junghans
Acquisition of data (provided animals, acquired and managed patients, provided facilities, etc.): S.C. Katz, R.A. Burga, L.J. Wang, W. Mooring, G. Point, P.D. Khare, Q. Ma, B.F. Stainken, E.O. Assanah, R. Davies, N.J. Espat, R.P. Junghans
Analysis and interpretation of data (e.g., statistical analysis, biostatistics, computational analysis): S.C. Katz, R.A. Burga, G. Point, P.D. Khare, M. Thorn, E.O. Assanah, N.J. Espat, R.P. Junghans
Writing, review, and/or revision of the manuscript: S.C. Katz, R.A. Burga, E. McCormack, P.D. Khare, M. Thorn, Q. Ma, B.F. Stainken, E.O. Assanah, R.P. Junghans
Administrative, technical, or material support (i.e., reporting or organizing data, constructing databases): S.C. Katz, R.P. Junghans
Study supervision: S.C. Katz, N.J. Espat, R.P. Junghans
Other (medical monitor): E. McCormack

Acknowledgments

The authors thank Dr. Michael Choi for his assistance with interpretation of the histology and immunohistochemistry data and Matthew Au at Boston University's Analytical Core for performing PCR. The authors also thank Dr. David Goldenberg and Dr. Hans Hansen of Immunomedics, Inc. for the supply of WI2 antibody for CAR-T detection and for the humanized anti-CEA MN14 antibody used for the creation of the chimeric antigen receptor of this study. The clinical trial was also supported by Prometheus Laboratories Inc. and Novartis Corporation with a grant-in-kind of PROLEUKIN® (IL2).

Grant Support

This study was financially supported by the NIH (1K08CA160662-01A1), the Society of Surgical Oncology Clinical Investigator Award supported by an education grant for Genentech, and the Rhode Island Foundation.

The costs of publication of this article were defrayed in part by the payment of page charges. This article must therefore be hereby marked *advertisement* in accordance with 18 U.S.C. Section 1734 solely to indicate this fact.

Received June 6, 2014; revised March 17, 2015; accepted March 23, 2015; published OnlineFirst April 7, 2015.

References

1. Katz SC, Bamboat ZM, Maker AV, Shia J, Pillarisetty VG, Yopp AC, et al. Regulatory T cell infiltration predicts outcome following resection of colorectal cancer liver metastases. Ann Surg Oncol 2013;20:946–55.
2. Katz SC, Donkor C, Glasgow K, Pillarisetty VG, Gonen M, Espat NJ, et al. T cell infiltrate and outcome following resection of intermediate-grade primary neuroendocrine tumours and liver metastases. HPB (Oxford) 2010;12:674–83.
3. Katz SC, Pillarisetty V, Bamboat ZM, Shia J, Hedvat C, Gonen M, et al. T cell infiltrate predicts long-term survival following resection of colorectal cancer liver metastases. Ann Surg Oncol 2009;16:2524–30.
4. Wagner P, Koch M, Nummer D, Palm S, Galindo L, Autenrieth D, et al. Detection and functional analysis of tumor infiltrating T-lymphocytes (TIL) in liver metastases from colorectal cancer. Ann Surg Oncol 2008;15:2310–7.
5. Turcotte S, Katz SC, Shia J, Jarnagin WR, Kingham TP, Allen PJ, et al. Tumor MHC class I expression improves the prognostic value of T-cell density in resected colorectal liver metastases. Cancer Immunol Res 2014;2:530–7.
6. Cantor HM, Dumont AE. Hepatic suppression of sensitization to antigen absorbed into the portal system. Nature 1967;215:744–5.
7. Katz SC, Pillarisetty VG, Bleier JI, Kingham TP, Chaudhry UI, Shah AB, et al. Conventional liver CD4 T cells are functionally distinct and suppressed by environmental factors. Hepatology 2005;42:293–300.
8. Katz SC, Pillarisetty VG, Bleier JI, Shah AB, DeMatteo RP. Liver sinusoidal endothelial cells are insufficient to activate T cells. J Immunol 2004;173:230–5.
9. Katz SC, Ryan K, Ahmed N, Plitas G, Chaudhry UI, Kingham TP, et al. Obstructive jaundice expands intrahepatic regulatory T cells, which impair liver T lymphocyte function but modulate liver cholestasis and fibrosis. J Immunol 2011;187:1150–6.
10. Grupp SA, Kalos M, Barrett D, Aplenc R, Porter DL, Rheingold SR, et al. Chimeric antigen receptor-modified T cells for acute lymphoid leukemia. N Engl J Med 2013;368:1509–18.
11. Porter DL, Levine BL, Kalos M, Bagg A, June CH. Chimeric antigen receptor-modified T cells in chronic lymphoid leukemia. N Engl J Med 2011;365:725–33.
12. Sadelain M, Brentjens R, Riviere I. The promise and potential pitfalls of chimeric antigen receptors. Curr Opin Immunol 2009;21:215–23.
13. Ma Q, Gonzalo-Daganzo R, Junghans RP. Genetically engineered T cells as adoptive immunotherapy of cancer. In:Giaccone G, Schilsky R, Sondel P, editors. Cancer Chemotherapy & Biological Response Modifiers: Elsevier Science; Philadelphia, PA, 2002. p. 319–45.
14. Park TS, Rosenberg SA, Morgan RA. Treating cancer with genetically engineered T cells. Trends Biotechnol 2011;29:550–7.
15. Ma Q, Gomes EM, Lo AS, Junghans RP. Advanced generation anti-prostate specific membrane antigen designer T cells for prostate cancer immunotherapy. Prostate 2014;74:286–96.
16. Blumenthal RD, Leon E, Hansen HJ, Goldenberg DM. Expression patterns of CEACAM5 and CEACAM6 in primary and metastatic cancers. BMC Cancer 2007;7:2.
17. Midiri G, Amanti C, Benedetti M, Campisi C, Santeusanio G, Castagna G, et al. CEA tissue staining in colorectal cancer patients. A way to improve the usefulness of serial serum CEA evaluation. Cancer 1985;55:2624–9.
18. Emtage PC, Lo AS, Gomes EM, Liu DL, Gonzalo-Daganzo RM, Junghans RP. Second-generation anti-carcinoembryonic antigen designer T cells resist activation-induced cell death, proliferate on tumor contact, secrete cytokines, and exhibit superior antitumor activity in vivo: a preclinical evaluation. Clin Cancer Res 2008;14:8112–22.
19. Parkhurst MR, Yang JC, Langan RC, Dudley ME, Nathan DA, Feldman SA, et al. T cells targeting carcinoembryonic antigen can mediate regression of metastatic colorectal cancer but induce severe transient colitis. Mol Ther 2011;19:620–6.
20. Kemeny NE, Melendez FD, Capanu M, Paty PB, Fong Y, Schwartz LH, et al. Conversion to resectability using hepatic artery infusion plus systemic chemotherapy for the treatment of unresectable liver metastases from colorectal carcinoma. J Clin Oncol 2009;27:3465–71.
21. Keilholz U, Scheibenbogen C, Brado M, Georgi P, Maclachlan D, Brado B, et al. Regional adoptive immunotherapy with interleukin-2 and lymphokine-activated killer (LAK) cells for liver metastases. Eur J Cancer 1994;30A:103–5.
22. Kobari M, Egawa S, Shibuya K, Sunamura M, Saitoh K, Matsuno S. Effect of intraportal adoptive immunotherapy on liver metastases after resection of pancreatic cancer. Br J Surg 2000;87:43–8.
23. Komatsu T, Yamauchi K, Furukawa T, Obata H. Transcatheter arterial injection of autologous lymphokine-activated killer (LAK) cells into patients with liver cancers. J Clin Immunol 1990;10:167–74.
24. Matsuhashi N, Moriyama T, Nakamura I, Ishikawa T, Ohnishi S, Nakagama H, et al. Adoptive immunotherapy of primary and metastatic liver cancer via hepatic artery catheter. Eur J Cancer 1990;26:1106–7.
25. Melichar B, Touskova M, Blaha M, Vesely P, Dvorak J, Krajina A, et al. Hepatic arterial administration of activated leukocytes in patients with liver metastases. Cancer Biother Radiopharm 2002;17:545–52.
26. Wolchok JD, Hoos A, O'Day S, Weber JS, Hamid O, Lebbe C, et al. Guidelines for the evaluation of immune therapy activity in solid tumors: immune-related response criteria. Clin Cancer Res 2009;15:7412–20.
27. Beaudoin EL, Bais AJ, Junghans RP. Sorting vector producer cells for high transgene expression increases retroviral titer. J Virol Methods 2008;148:253–9.

28. Quintas-Cardama A, Yeh RK, Hollyman D, Stefanski J, Taylor C, Nikhamin Y, et al. Multifactorial optimization of gammaretroviral gene transfer into human T lymphocytes for clinical application. Hum Gene Ther 2007; 18:1253–60.
29. Karimi MA, Lee E, Bachmann MH, Salicioni AM, Behrens EM, Kambayashi T, et al. Measuring cytotoxicity by bioluminescence imaging outperforms the standard chromium-51 release assay. PLoS ONE 2014;9:e89357.
30. Junghans RP, Manning W, Safar M, Quist W. Biventricular cardiac thrombosis during interleukin-2 infusion. N Engl J Med 2001;344:859–60.
31. Mocellin S, Pilati P, Lise M, Nitti D. Meta-analysis of hepatic arterial infusion for unresectable liver metastases from colorectal cancer: the end of an era? J Clin Oncol 2007;25:5649–54.
32. Takayama T, Sekine T, Makuuchi M, Yamasaki S, Kosuge T, Yamamoto J, et al. Adoptive immunotherapy to lower postsurgical recurrence rates of hepatocellular carcinoma: a randomised trial. Lancet 2000;356:802–7.
33. Rosenberg SA, Yang JC, Schwartzentruber DJ, Hwu P, Marincola FM, Topalian SL, et al. Prospective randomized trial of the treatment of patients with metastatic melanoma using chemotherapy with cisplatin, dacarbazine, and tamoxifen alone or in combination with interleukin-2 and interferon alfa-2b. J Clin Oncol 1999;17:968–75.
34. Lo AS, Ma Q, Liu DL, Junghans RP. Anti-GD3 chimeric sFv-CD28/T-cell receptor zeta designer T cells for treatment of metastatic melanoma and other neuroectodermal tumors. Clin Cancer Res 2010;16: 2769–80.
35. Bramswig KH, Poettler M, Unseld M, Wrba F, Uhrin P, Zimmermann W, et al. Soluble carcinoembryonic antigen activates endothelial cells and tumor angiogenesis. Cancer Res 2013;73:6584–96.
36. Takayama T, Makuuchi M, Sekine T, Terui S, Shiraiwa H, Kosuge T, et al. Distribution and therapeutic effect of intraarterially transferred tumor-infiltrating lymphocytes in hepatic malignancies. A preliminary report. Cancer 1991;68:2391–6.
37. Kooreman NG, Ransohoff JD, Wu JC. Tracking gene and cell fate for therapeutic gain. Nat Mater 2014;13:106–9.
38. Saied A, Licata L, Burga RA, Thorn M, McCormack E, Stainken BF, et al. Neutrophil:lymphocyte ratios and serum cytokine changes after hepatic artery chimeric antigen receptor-modified T-cell infusions for liver metastases. Cancer Gene Ther 2014;21:457–62.
39. Hansen HJ, Goldenberg DM, Newman ES, Grebenau R, Sharkey RM. Characterization of second-generation monoclonal antibodies against carcinoembryonic antigen. Cancer 1993;71:3478–85.
40. Scheinberg DB, Mulford DA, Jurcic JG, Sgouros G, Junghans RP. Antibody-based therapies for cancer. In:Chabner BA, Longo DL, editors. Cancer Chemotherapy and Biotherapy. 4th ed; Lippincott, Williams, and Wilkins; Philadelphia, PA, 2006. p. 666–98.
41. Dudley ME, Yang JC, Sherry R, Hughes MS, Royal R, Kammula U, et al. Adoptive cell therapy for patients with metastatic melanoma: evaluation of intensive myeloablative chemoradiation preparative regimens. J Clin Oncol 2008;26:5233–9.
42. Lotze MT, Matory YL, Ettinghausen SE, Rayner AA, Sharrow SO, Seipp CA, et al. In vivo administration of purified human interleukin 2. II. Half life, immunologic effects, and expansion of peripheral lymphoid cells in vivo with recombinant IL 2. J Immunol 1985;135:2865–75.
43. Gershwin M.E. VJM, Manns M.P. Liver Immunology. 1st ed. Philadelphia: Hanley & Belfus, Inc.; 2003.
44. Pillarisetty VG, Shah AB, Miller G, Bleier JI, DeMatteo RP. Liver dendritic cells are less immunogenic than spleen dendritic cells because of differences in subtype composition. J Immunol 2004;172:1009–17.
45. Brahmer JR, Tykodi SS, Chow LQ, Hwu WJ, Topalian SL, Hwu P, et al. Safety and activity of anti-PD-L1 antibody in patients with advanced cancer. N Engl J Med 2012;366:2455–65.
46. Topalian SL, Hodi FS, Brahmer JR, Gettinger SN, Smith DC, McDermott DF, et al. Safety, activity, and immune correlates of anti-PD-1 antibody in cancer. N Engl J Med 2012;366:2443–54.
47. Porter DL, Levine BL, Bunin N, Stadtmauer EA, Luger SM, Goldstein S, et al. A phase 1 trial of donor lymphocyte infusions expanded and activated ex vivo via CD3/CD28 costimulation. Blood 2006;107:1325–31.